Coarsening Dynamics of Umbilical Defects in Inhomogeneous Medium

Raouf Barboza, Umberto Bortolozzo, Marcel G. Clerc, Stefania Residori and Valeska Zambra

Abstract Non-equilibrium systems with coexistence of equilibria exhibit a rich and complex defects dynamics in order to reach a more stable configuration. Nematic liquid crystals layer with negative dielectric constant and homeotropic anchoring under the influence of a voltage are the ideal context for studying the interaction of gas of topological vortices. The number of vortices decreases with time. Experimentally, we show that the presence of imperfections drastically changes this coarsening law. Imperfections are achieved by considering glass beads inside the nematic liquid crystal sample. Depending on the disorder of these imperfections, the system exhibits different statistical evolution of the number of umbilical defects. The coarsening dynamics is persistent and is characterized by power laws with different exponents.

1 Introduction

Macroscopic systems under the influence of injection and dissipation of energy and momenta exhibit instabilities leading to spontaneous symmetry breaking and pattern

R. Barboza (✉) · M.G. Clerc
Departamento de Física, Facultad de Ciencias Físicas Y Matemáticas,
Universidad de Chile, Casilla 487-3, Santiago, Chile
e-mail: raouf.barboza@ing.uchile.cl

M.G. Clerc
e-mail: marcel@dfi.uchile.cl

U. Bortolozzo · S. Residori
Institut Nonlinéaire de Nice, Université de Nice-Sophia Antipolis, CNRS,
1361 Route des Lucioles, 06560 Valbonne, France
e-mail: umberto.bortolozzo@inln.cnrs.fr

S. Residori
e-mail: stefania.residori@inln.cnrs.fr

V. Zambra
Departamento de Física, Facultad de Ciencias, Universidad de Chile, Santiago, Chile
e-mail: valesk.za@gmail.com

M. Tlidi and M.G. Clerc (eds.), *Nonlinear Dynamics: Materials, Theory and Experiments*, Springer Proceedings in Physics 173,
DOI 10.1007/978-3-319-24871-4_2

formation [1]. Due to the inherent fluctuations of these macroscopic systems, different organizations may emerge in distinct regions of the same sample; hence, these spatial structures are usually characterized by domains, separated by interfaces, as grain boundaries, and defects or dislocations [2, 3]. Among others, defects in rotationally invariant two dimensional systems, i.e. vortices, attract a great deal of attention because of their universal character and intriguing topological properties. These defects have been observed in different systems such as fluids, superfluids, superconductors, liquid crystals, fluidized anisotropic granular matter, magnetic media, and optical dielectrics, to mention a few [4]. Vortices occur in complex fields and can be identified as topological defects, that is, point-like singularities which locally break rotational symmetry. They exhibit a zero intensity at the singular point with a phase spiraling around it. The topological charge is assigned by counting the number of spiral arms in the phase distribution, while the sign is given by the sense of the spiral rotation.

Nematic liquid crystals with negative anisotropic dielectric constant and homeotropic anchoring are a natural physical context where dissipative vortices can be observed and analyzed [5, 6]. In this context, the dissipative vortices are usually called umbilical defects. These defects in nematic liquid crystals have long been reported in the literature (see textbooks [5–7] and reference therein). Two types of stable vortices with opposite charges are observed, which are characterized by being attracted to (repelled by) the opposite (identical) topological charge. The nematic liquid crystal phase is characterized by rod-shaped molecules that have no positional order but tend to point in the same direction [5–7]. Then, the description of the nematic liquid crystal is given by a vector—the director $\mathbf{n}$—which accounts for the molecular orientational order. The direction of this vector is irrelevant, only the orientation of $\mathbf{n}$ has a physical meaning. Note that the defects observed in this context are similar to those observed in magnetic systems, superfluids, superconductors, and Bose-Einstein condensates. However, these vortices exhibit a entirely different dynamic evolution due to the strongly dissipative nature of liquid crystals.

The vortex-like defects have accompanied liquid crystals since their discovery in 1889 by Lehmann [8], who called these structures *kernel*. Later, they were observed in a similar experimental setup by Friedel, who called them *noyaux* [9]. Moreover, he also resolved their detailed topological structure. From the theory of elasticity of nematic liquid crystals, Frank calculated the detailed structure of these defects [10]. Due to the fact that these defects break the orientational order and by analogy with dislocations in crystals of condensed matter, Frank called these defects *disclinations*. Despite the different names given to the observed vortices in this context, none of them were adopted by the community of liquid crystals. There the most widely used name for these defects is *nematic umbilical defects*. The term umbilics was coined by Rapini [11] and refers to the topological structure of the defect which corresponds to a string-like object in three dimensions. Because of the complex elasticity theory associated with nematic liquid crystals, characterized by three types of deformation (bend, twist and splay), the theoretical dynamic study of defects is a thorny task [5–7].

Based on weak nonlinear analysis, valid close to the orientational instability of the molecules (Fréedericksz transition [5, 6]), the dynamics of the director can be reduced at main order to the Ginzburg-Landau equation with real coefficients [12–14]. This amplitude equation allows to understand the emergence of different orientational domains, two types of stable vortices and their respective dynamics. Since the vortices have a $\pm 2\pi$ azimuthal phase jump (winding number), usually they are referred to as vortex "+" and "−", respectively. In this approach, both defects are indistinguishable in their amplitude and, as a result of the phase invariance of the Ginzburg-Landau equation, they account for a continuous family of solutions, characterized by a phase parameter [4]. From this model one can characterize the interaction of vortex pairs [4], which shows a good agreement with experimental observations [15]. From the interaction of defect pairs and through the use of self similarity statements, one can infer the law of number of defects as a function of time [16, 17]. This type of self-similar behavior is well-known as *coarsening process*, which is equivalent to the growth process of domains in phase separations transitions observed in metallic alloys [18]. Using the law of vortices interaction, one shows that the number of defects decreases inversely proportional to time, which it has been experimentally observed in nematic liquid crystal samples [19, 20]. Similarly, using XY phase model, one obtains the same decay law for the vortices number [19].

The aim of this manuscript is to investigate experimentally the persistence and coarsening law when inhomogeneities are considered in a liquid crystal sample. The inhomogeneities are achieved by considering glass beads inside a nematic liquid crystals sample with negative dielectric constant and homeotropic anchoring. Depending on the disorder of these glass beads, the system exhibits different statistical temporal evolution of number of umbilical defects. This evolution is found to exhibit power laws with different exponents.

2 Experimental Setup

Let us consider an interaction geometry in which, a uniform thin layer of nematic liquid crystal has the molecular director constrained to be normal to the two parallel bounding plates, direction which we later denote by z. Due to inherent elastic forces between the molecules, the alignment in the bulk will be uniform and parallel to z, this in order to minimize the elastic energy. When a low frequency ($\approx$100 kHz in our case) electric field is applied in the z direction, if the dielectric anisotropy of the liquid crystal is negative, the resulting electric torque will try to rotate the molecules away from the z-axis. Only over a critical threshold voltage, called Fréedericksz transition voltage [6], the molecules effectively tilt away from their equilibrium position. Due to the 2π degeneracy in the possible direction of orientation, defects called umbilics will be generated in the nematic layer [6, 11].

The observation of these umbilical defects and their dynamics was done by using two different types of liquid crystal cells about the same thickness. The first cell, uniform, is made of two ITO (Indium Tin Oxide, transparent conductor) coated glass

Fig. 1 Sketch of the experimental setup of a nematic liquid crystal layer with negative dielectric constant anisotropy and homeotropic anchoring under the influence of a voltage. The essential parts of the setup are emphasized. Crossed polarizers, either linear or circular are used to analyze the texture of the liquid crystal

slabs. The glass slabs are treated on the ITO side in order to promote orthogonal alignment of the liquid crystal molecules. This alignment is termed as homeotropic alignment or homeotropic anchoring [5–7]. The glass slabs are held together with thin sheet of polymer spacers such that, the treated faces form a gap in which the liquid crystal will be infiltrated later. The spacers, which fix the thickness of the gap are about 15 μm thick. The second cell, non uniform, from Instec Inc. (SB100A150uT180 liquid crystal cell), has the same homeotropic alignment. The spacing gap of the cell is achieved by sputtering spacer beads made of clear/transparent ceramics or glass onto the substrate of glass slab before assembly [21]. The diameter of these glass micro-spheres fixes the cell gap, and, for the chosen cell, it is about 15 μm. The two cells were filled by capillarity with the MLC-6608 nematic liquid crystal (from Merck) which has a negative dielectric anisotropy. Both cells are biased with low frequency sinusoidal voltage. The experimental setup is sketched in the figure Fig. 1. To achieve maximum resolution, a collimated white light (Köhler illumination) from a microscope condenser is sent onto the liquid crystal cell, the latter mounted on a translation stage. The texture of the liquid crystal is imaged on a CCD camera through a microscope objective and relay lenses.

As the cells contain liquid crystalline materials, which are an intrinsically birefringent in the nematic phase, two crossed polarizers, the first to polarize the illumination source and the second to analyze the polarization of the light coming from the cell, are used in order to recover averaged two dimensional texture of the liquid crystal layer. For simplicity the cell will be considered as a uniform, along the longitudinal z coordinate, uniaxial birefringent material with optical axis aligned in the xy plane at angle θ with the x axis, with retardation $\delta = 2\pi L(\tilde{n}_e - n_o)/\lambda$; L represents the thickness of the cell, λ the operating wavelength, n_o and $\tilde{n}_e$ respectively the ordinary refractive index and the average extraordinary refractive index over the longitudinal coordinate. The optical axis can be viewed as the averaged azimuthal direction of molecules in the xy plane, equivalently their projection onto the xy plane. The averaged extraordinary index $\tilde{n}_e$ is related to the tilt ψ of the molecules with respect the z axis by the expression

$$\tilde{n}_e = \int_0^L \frac{n_e n_o}{\sqrt{n_e^2 \cos^2 \psi + n_o^2 \sin^2 \psi}} dz. \tag{1}$$

The texture of the liquid crystal layer will vary accordingly with the spatial variation in the xy optical axis at angle θ representing the director orientation in the xy plane and δ the retardation which depends on the average tilt ψ of the molecules with respect to the z axis. Using Jones matrix formalism we can show that the intensity recorded using crossed linear polarizers, the polarizers axis are perpendicular to each other, is given by

$$I(x, y) = I_0 \sin^2 \frac{\delta(x, y)}{2} \sin^2 2\theta(x, y). \tag{2}$$

Likewise, the crossed circular polarizer configuration is achieved when two quarter wave plate (QWP) are inserted in the previous configuration, with the first waveplate at $\pm 45°$ with respect to the axis of the input polarizer, and the fast axis of the second wave-plate is orthogonal to the first one. In this case the recorded intensity writes as follow

$$I(x, y) = I_0 \sin^2 \frac{\delta(x, y)}{2} \tag{3}$$

We used both polarizing microscope imaging, depending on the feature we want to enhance of the umbilical defects dynamics.

3 Results and Discussions

To understand the coarsening dynamics of the vortices in homogeneous cell, we must first establish the vortex pair interaction law and then, by means of self-similarity properties, we can deduce a coarsening law of vortices.

3.1 Vortex-Pair Interaction Law

As we have mention before, close to the orientational instability of the molecules, the dynamics of the director can be reduced at main order to the Ginzburg-Landau equation with real coefficients. This amplitude equation admits stable vortex solutions with topological charge ± 1. The analysis of the vortex interaction law is complex because the energy associated with each vortex diverges logarithmically with the size of the system [5]. Thereby, the interaction between distant vortices has an infinite mobility [4]. However, in the case of considering that the system has a finite size, the mobility is finite and the vortex-pair interaction law can be approximated for long distances by the expression [4]

$$M\dot{r} = \frac{q}{r}, \tag{4}$$

where $r(t)$ is the vortex separation, q is the product of the topological charges of vortices ($q = \pm 1$), then it is positive (negative) when both vortex has the same (different) charge, and M stands for the vortex mobility which depends of the size of the system, the properties of the liquid crystal and the applied voltage. Thus the interaction between vortices is equivalent to overdamped particles with Keplerian type interaction potential. When the distances between the vortices is small enough—the order of the size of the vortex core—the previous dynamics is not valid. But in this case, vortices of opposite charge merge and disappear. In brief, the dynamics of interaction between vortices tries to homogenize the deformations of molecular orientation.

3.2 Vortex Coarsening Law

Considering a gas of n-vortices, the position of the ith-vortex is given by $\mathbf{r}_i$. Hence, the interaction between them is given by

$$M\dot{\mathbf{r}}_i = \sum_{i \neq j} \frac{q_{ij}}{r_{ij}^2}(\mathbf{r}_i - \mathbf{r}_j), \tag{5}$$

where $r_{ij} \equiv ||\mathbf{r}_i - \mathbf{r}_j||$ is the distance between the ith and jth-vortex, and q_{ij} is the product of the topological charges of vortices. Hence, the dynamics of a gas of n-vortices corresponds to overdamped n-body problem. It is worthy to note the above set of equations is invariant under the self-similarity transformation

$$\begin{aligned} \mathbf{r}_i &\rightarrow \lambda \mathbf{r}_i, \\ t &\rightarrow \lambda^2 t. \end{aligned} \tag{6}$$

Therefore, if one dilates or expands the space and time then the set of (5) are invariant.

Let us introduce $N(t)$, the number of vortices at time t. This number of vortices can be estimated as

$$N(t) = \frac{A}{\langle r \rangle^2}, \tag{7}$$

where A is the area of the sample under study and $\langle r \rangle$ is the average distance between vortices. Because the dynamics of vortices is given by the set of (5), also the average distance $\langle r \rangle$ and $N(t)$ is determined by this dynamics. Then, $\langle r \rangle$ and $N(t)$ should also be self similar with transformation (6). Hence, $N(\lambda^2 t) = A/\lambda\langle r\rangle^2$. From the previous equality, one infers that the only possibility is that

$$N(t) = \frac{\beta}{t}, \tag{8}$$

with β a constant. Therefore, the number of defects decreases inversely proportional to time, *coarsening law*.

3.3 Experimental Observation of Coarsening Law in Uniform Cell

To verify the previous law, we have conducted several experimental analysis of the dynamics of vortex gas. This by applying a large enough voltage to the liquid crystal layer between two cross polarizers, which spontaneously generates hundreds umbilical defects in different positions as a result of thermal fluctuations and inhomogeneities in the system. The position of the umbilical defects are recognized by the intersection of four black curves [5]. Subsequently, the defects have a dynamic of attraction and repulsion following the interaction law (5). Figure 2 shows a temporal sequence of snapshots, which emphasizes the characteristic evolution of a gas of umbilical defects. From the temporal sequences and through an appropriate recognition software we can determine the number of vortices and their respective positions. Thus, we acquire the evolution of the number of vortices as a function of time. Figure 3 shows this evolution. From this plot, one concludes that the number of

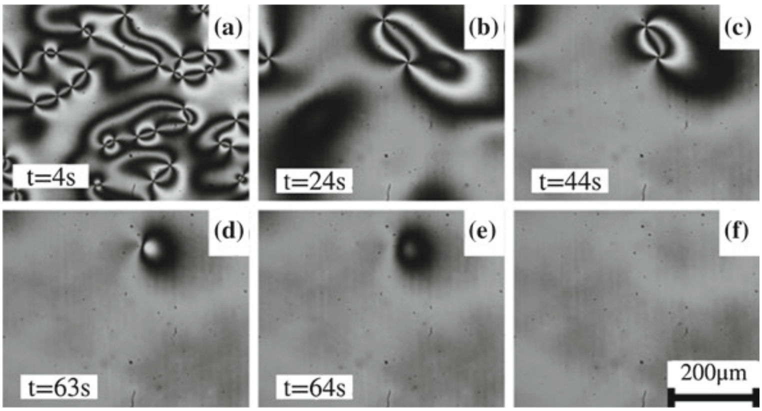

Fig. 2 Annihilation dynamics of umbilical defects in a uniform liquid crystal layer between two crossed linear polarizers. Temporal sequence of snapshots from the *left* to *right* and the *top* to *bottom* (**a**–**e**). The position of the umbilical defects are given by the intersection of four *black brushes*. Texture of the sample after the anihilation of all the defects (**f**)

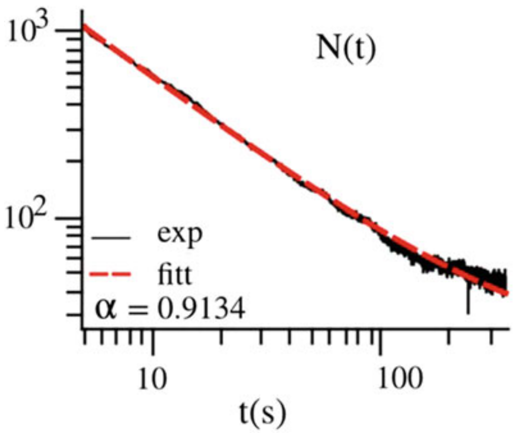

Fig. 3 Coarsening dynamics in a uniform cell. Number of umbilical defects as a function of time. The *solid black* and *dashed curve*, respectively, are the experimental evolution of $N(t)$ and the fitting *curve* $N_f(t) = \beta t^{-\alpha} + N_\infty$ with $\alpha = 0.9134 \pm 0.00124$, $\beta = 4.448 \times 10^3 \pm 10$ and $N_\infty = 17 \pm 0.22$

vortices decays as a function of time with a power law. To determine the exponent, we have considered the following fit

$$N_f(t) = \beta t^{-\alpha} + N_\infty, \tag{9}$$

where $\{\beta, \alpha, N_\infty\}$ are fitting parameters, which accounts for the features of the liquid crystal and cell under study. N_∞ stands for the number of imperfections of the system—which trap the vortices in given positions—and the inaccuracy of recognition method. Experimentally we found that in our samples, the exponent $\alpha = 0.9134$ is in reasonable agreement with the simplified description (5).

3.4 *Experimental Observation of Coarsening Law in Inhomogeneous Cell*

To investigate of the interaction of vortices in inhomogeneous media, we have conducted several experimental analysis of the dynamic of vortex gas in a liquid crystal layer with glass beads between two cross polarizers and applying a large enough voltage. Figure 4 shows a temporal sequence of snapshots with the characteristic evolution of a gas of umbilical defects in an inhomogeneous medium. The glass beads are emphasized by dashed circumferences. Again, the position of the umbilical defects are recognized by the intersection of four black curves. As we have observed in the temporal sequence of snapshots, when one applies a sufficiently large voltage in the liquid crystal layer a large number of vortices appear in different spatial positions, which are determined by the inherent fluctuations and imperfections in the cell. Following the emergence of these umbilical defects, they begin to repel or attract, causing the annihilation process of these defects. This process is characterized by the fact that initially close defects annihilate quickly, and then the more distant umbilical defects annihilate one another, but each time in a slower process, coarsening

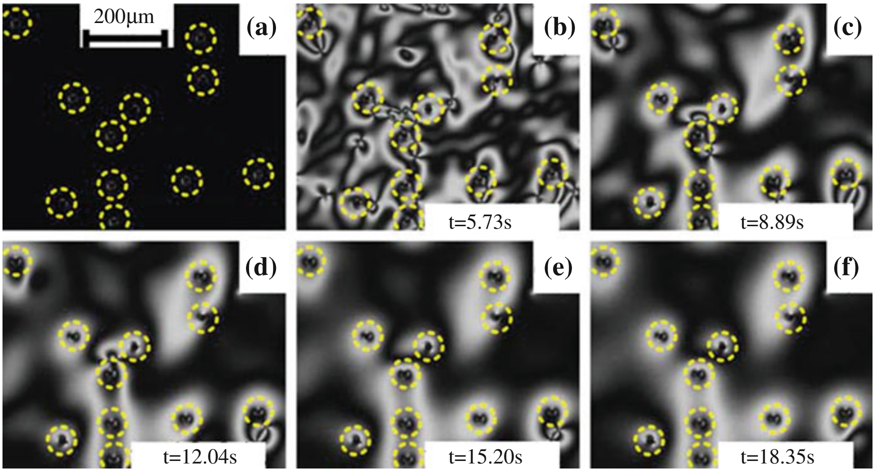

Fig. 4 Umbilical defects annihilation dynamics in a liquid crystal layer with glass beads between two linear crossed polarizers. Temporal sequence of snapshots from the *left* to *right*. The position of the umbilical defects are given by the intersection of four *black curves*

dynamics. The glass beads, as seen in the snapshots, remain motionless. However, the dynamics of vortices is strongly affected by the presence of glass beads. Figure 5 shows a glass bead attracting radially an umbilical defect . Both appear as dark spots as the cell is observed with circular crossed polarizers. In this experimental setup umbilical defects are recognized as small gray circles. Experimentally, this interaction is weaker than the interaction between umbilical defects. It is known that glass beads without surface treatment, generate homeotropic anchoring at their boundaries, that the liquid crystal molecules tend to be oriented normal to the glass beads [21, 22]. In addition, due to the fact that the glass beads are in contact with the glass plates of the sample, one expects a saturn ring like defect loop around each glass inclusion [21, 22]. The trajectory as consequence of the interaction between this defect and the umbilical one is depicted in Fig. 5. Likewise, the interactions between vortices are affected by the presence of the glass beads. Figure 6 illustrates the vortex interaction in presence of a close glass bead in a liquid crystal layer observed with circular crossed polarizers. Clearly from this trajectory, we note that the interaction of the umbilical defects is not a central force as those obtained by (4). Therefore, the interaction of vortices is modified and it is not clear if the process of coarsening is persistent.

Using an appropriate recognition software, based on particle tracking, we can determine the number of vortices and their respective positions. Figures 7c and 8c show the evolution of the number of umbilical defects as a function of time. In both graphs, we observe that the system exhibits coarsening process with power laws. These power laws are obtained by realizing several experiments. Hence, the coarsening dynamics is a persistent phenomenon, though depending on the distribution of the glass beads, we observe different power laws. To characterize the clustering

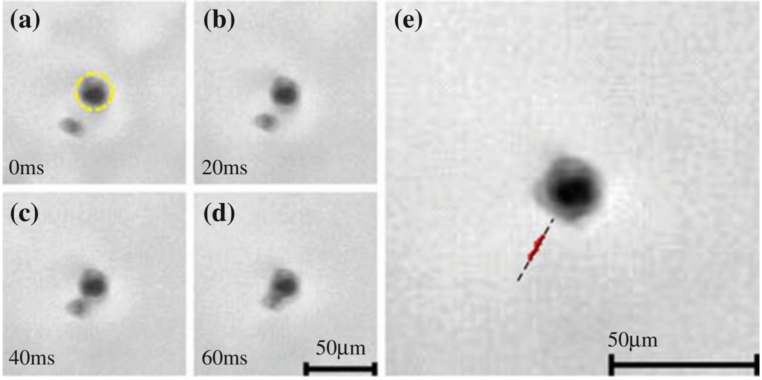

Fig. 5 Interaction between a glass bead and an umbilical defect in a liquid crystal layer with circular crossed polarizers. Temporal sequence of snapshots from (**a**) to (**e**). *Dashed circle* accounts for the glass bead. The small *gray circle* stands for the umbilical defect. In the *right panel*, the *dashed line* sums up the trajectory of the umbilical defect and points are the position of the defect

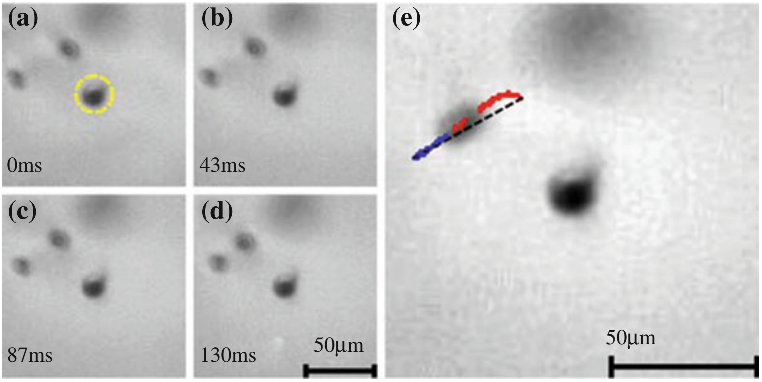

Fig. 6 Vortex interaction in presence of a glass bead in a liquid crystal layer with circular crossed polarizers. Temporal sequence of snapshots from (**a**) to (**e**). *Dashed circle* accounts for a glass bead. The small *gray circle* stands for the umbilical defects. In the *right panel*, the color points account for the trajectories of the umbilical defects, different colors account for the different defects, and the *dashed line* joints initially the defects

and distribution of the glass beads, we have computed the Voronoi diagram of glass beads in the different observed zones (cf. Figs. 7a and 8a) and their histogram of the mutual distance of the glass beads (cf. Figs. 7b and 8b). From these diagrams, we can measure the density of glass beads and we obtain for zone I and III, respectively, 13.630 and 20.803 glass beads per mm^2. Zone III is more ordered than zone I, since its histogram of the mutual distance is closer to a Rayleigh distribution around a length (cf. Fig. 7b) and the other is closer to a uniform distribution without a feature length. Analogously, from this distribution we can compute the Shannon entropy

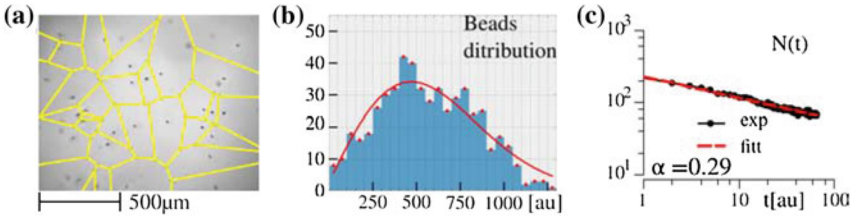

Fig. 7 Coarsening process of umbilical defects in an inhomogeneous medium, zone III. **a** Voronoi diagram of glass beads in the observed zone. **b** Histogram of the mutual distance of the glass beads. The *solid curve* is a fitting curve using a Rayleigh distribution. **c** Corresponding scaling curve of the number of defects vs normalized time. *Black* points stand for experimental observations and the *dashed line* corresponds to a fitting curve of the form $N(t) = \beta/t^{\alpha}$ with $\alpha = 0.29$

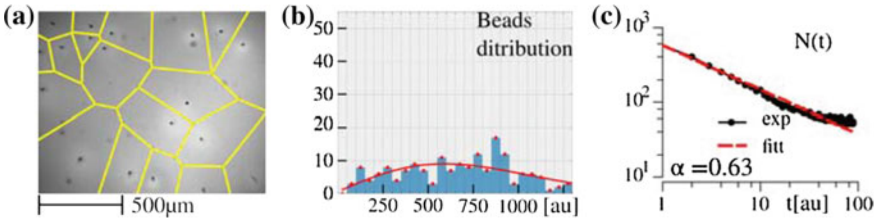

Fig. 8 Coarsening process of umbilical defects in an inhomogeneous medium, zone I. **a** Voronoi diagram of glass beads in the observed zone. **b** Histogram of the mutual distance of the glass beads. The *solid curve* is a *fitting curve* using a Rayleigh distribution. **c** Corresponding scaling *curve* of the number of defects vs normalized time. *Black* points stand for experimental observations and the *dashed line* corresponds to a *fitting curve* of the form $N(t) = \beta/t^{\alpha}$ with $\alpha = 0.63$

S_e and obtain for each zone, respectively $S_e(III) = 0.00767$ and $S_e(I) = 0.021$. Therefore, depending on the different configurations of the glass beads, the evolution of the number of defects as a function of time changes.

To measure the exponent of the coarsening laws, we have considered the following fitting curve $N(t) = \beta t^{-\alpha}$. Table 1 summarizes our results for different zones of our liquid crystal layer. Different zones of the sample exhibit different coarsening laws. However, from this table we are not able to establish a correlation between the

Table 1 Results over an observed area about 1.394 mm^2

Zone	Density (mm^2)	α	β	Entropy
I	13.630	0.63	597.0	0.0210
II	17.217	0.85	1800.0	0.0136
III	20.803	0.29	228.1	0.00767
IV	21.521	0.75	1286.0	0.0091
V	23.673	0.758	1286.0	0.00772
VI	27.977	0.73	187.0	0.0057

density of vortices, Shannon entropy, and spatial distributions with their coarsening exponents found experimentally.

4 Conclusions and Remarks

Far from equilibrium systems with coexistence of equilibria exhibit a rich and complex defects dynamics in order to reach a more stable configuration. This dynamic of defects can generate a rich variety of spatial textures. Defects in rotationally invariant two dimensional systems, attract a great deal of attention because of their universal character and intriguing topological properties. Nematic liquid crystals layer with negative dielectric constant and homeotropic anchoring under the influence of a voltage are the ideal context for studying the interaction of gas of topological vortices with opposite charges.

By considering a uniform sample of nematic liquid crystal layer under the influence of electrical voltage with high frequency, we observe that the number of vortices decrease inversely proportional to time. This coarsening dynamics results when vortices are more close, the interaction between them increases in a self-similarity manner. Experimentally, we show that the presence of imperfections in the liquid crystal layer drastically changes this coarsening process. Imperfections are achieved by considering glass beads inside the nematic liquid crystal sample. We observed that the coarsening process is persistent under the presence of spatial inhomogeneities. Depending on the disorder of these imperfections, the system exhibits different statistical evolution of number of umbilical defects. This evolution is characterized by power laws with different exponents.

From the theoretical point of view, one can model the effect of the glass beads as a screening effect, that is, the law of interaction of pairs of vortices, (4), is modified by considering an effective exponent, which is a function of the properties and distributions of the glass beads. This kind of effective dynamic is self-similar, then this could explain the observed coarsening dynamics.

Acknowledgments M.G.C. acknowledges the support of FONDECYT N 1150507. R.B. acknowledges the support of FONDECYT POSTDOCTORADO N. 3140577.

References

1. G. Nicolis, I. Prigogine, *Self-Organization in Non Equilibrium Systems* (Wiley, New York, 1977)
2. L.M. Pismen, *Patterns and Interfaces in Dissipative Dynamics* (Springer Series in Synergetics, Berlin, 2006)
3. M.C. Cross, P.C. Hohenberg, Pattern formation outside of equilibrium. Rev. Mod. Phys. **65**, 851–1112 (1993)
4. L.M. Pismen, *Vortices in Nonlinear Fields* (Clarendon press, Oxford, 1999)

5. S. Chandrasekhar, Liquid Crystals (Cambridge University Press, Cambridge, 1992)
6. P.G. de Gennes, J. Prost, The physics of Liquid Crystals, 2nd edn. (Oxford Science Publications, Clarendon Press, Oxford, 1993)
7. P. Oswald, P. Pieranski, Nematic and Cholesteric Liquid Crystals (Taylor & Francis Group, Boca Raton, 2005)
8. O. Lehmann, Über fliessende krystalle. Zeitsch Phys. Chem. 4, 462-472 (1889)
9. G. Friedel, The mesomorphic states of matter. Ann. Physique **18**, 273–474 (1922)
10. F.C. Frank, I. Liquid crystals. On the theory of liquid crystals. Discuss. Faraday Soc. 25, 19-28 (1958)
11. A. Rapini, Umbilics: static properties and shear-induced displacements. J. Physique **34**, 629–633 (1973)
12. T. Frisch, S. Rica, P. Coullet, J.M. Gilli, Spiral waves in liquid crystal. Phys. Rev. Lett. **72**, 1471–1474 (1994)
13. T. Frisch, Spiral waves in nematic and cholesteric liquid crystals. Phys. D **84**, 601–614 (1995)
14. M.G. Clerc, E. Vidal-Henriquez, J.D. Davila, M. Kowalczyk, Symmetry breaking of nematic umbilical defects through an amplitude equation. Phys. Rev. E **90**, 012507 (2014)
15. R. Barboza, T. Sauma, U. Bortolozzo, G. Assanto, M.G. Clerc, S. Residori, Characterization of the vortex-pair interaction law and nonlinear mobility effects. New J. Phys. **15**, 013028 (2013)
16. M. Argentina, M.G. Clerc, R. Rojas, E. Tirapegui, Coarsening dynamics of the one-dimensional Cahn-Hilliard model. Phys. Rev. E **71**, 046210 (2005)
17. M.G. Clerc, S. Coulibaly, L. Gordillo, N. Mujica, R. Navarro, Coalescence cascade of dissipative solitons in parametrically driven systems. Phys. Rev. E **84**, 036205 (2011)
18. L. Ratke, P.W. Voorhees, Growth and Coarsening: Ostwald Ripening in Material Processing (Springer Science and Business Media, 2013)
19. A.N. Pargellis, S. Green, B. Yurke, Planar XY-model dynamics in a nematic liquid crystal system. Phys. Rev. E 49, 42504257 (1994)
20. T. Nagaya, H. Orihara, Y. Ishibashi, Coarsening dynamics of +1 and -1 disclinations in two-dimensionally aligned nematics-spatial distribution of disclinations. J. Phys. Soc. Japan, 64, 7885 (1995)
21. M. Hasegawa, Alignment Technology and Applications of Liquid Crystal Devices (CRC Press), pp. 7–54
22. H. Stark, Director field configurations around a spherical particle in a nematic liquid crystal. Eur. Phys. J. B 10, 311321 (1999)

http://www.springer.com/978-3-319-24869-1

Nonlinear Dynamics: Materials, Theory and Experiments
Selected Lectures, 3rd Dynamics Days South America, Valparaiso 3-7 November 2014
Tlidi, M.; Clerc, M.G. (Eds.)
2016, XV, 361 p. 164 illus., 114 illus. in color., Hardcover
ISBN: 978-3-319-24869-1